THE JOURNAL OF PHYSICAL CHEMISTRY B

Article

pubs.acs.org/JPCB

Driving Mechanisms of Ionic Polymer Actuators Having Electric Double Layer Capacitor Structures

Satoru Imaizumi, Yuichi Kato, Hisashi Kokubo, and Masayoshi Watanabe*

Department of Chemistry and Biotechnology, Yokohama National University, 79-5 Tokiwadai, Hodogaya-ku, Yokohama 240-8501, Japan

Supporting Information

ABSTRACT: Two solid polymer electrolytes, composed of a polyether-segmented polyurethaneurea (PEUU) and either a lithium salt (lithium bis(trifluoromethanesulfonyl)amide: Li[NTf_2]) or a nonvolatile ionic liquid (1-ethyl-3-methylimidazolium bis(trifluoromethanesulfonyl)amide: [C_2mim][NTf_2]), were prepared in order to utilize them as ionic polymer actuators. These salts were preferentially dissolved in the polyether phases. The ionic transport mechanism of the polyethers was discussed in terms of the diffusion coefficients and ionic transference numbers of the incorporated ions, which were estimated by means of pulsed-field gradient spin−echo (PGSE) NMR. There was a distinct difference in the ionic transport properties of each polymer electrolyte owing to the difference in the magnitude of interactions between the cations and the polyether. The anionic diffusion coefficient was much faster than that of the cation in the polyether/Li[NTf_2] electrolyte, whereas the cation diffused faster than the anion in the polyether/[C_2mim][NTf_2] electrolyte. Ionic polymer actuators, which have a solid-state electric-double-layer-capacitor (EDLC) structure, were prepared using these polymer electrolyte membranes and ubiquitous carbon materials such as activated carbon and acetylene black. On the basis of the difference in the motional direction of each actuator against applied voltages, a simple model of the actuation mechanisms was proposed by taking the difference in ionic transport properties into consideration. This model discriminated the behavior of the actuators in terms of the products of transference numbers and ionic volumes. The experimentally observed behavior of the actuators was successfully explained by this model.

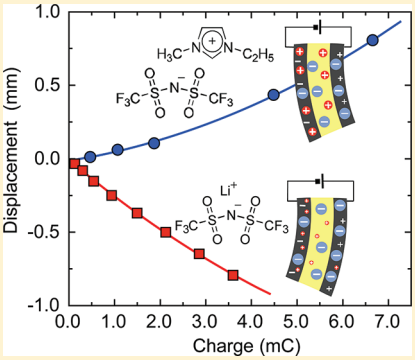

INTRODUCTION

Polymer actuators, especially electroactive polymer (EAP) actuators, are expected to be the next generation of driving parts because they have nonconventional features such as soft motion, lightweight, and ease and flexibility of processing.[1−6] Ionic EAP actuators in particular, which are a subclass of EAP actuators and are driven by migration or diffusion of ions, exhibit large deformation with low voltage (<5 V) applications, as seen in conducting polymer actuators,[4] ionic-polymer metal composites,[5] and carbon nanotube actuators.[6] However, conventional ionic EAP actuators suffer a drawback in durability under open atmosphere owing to the evaporation of solvents contained in the polymer electrolytes, which are essential for the movement of ions. Moreover, the narrow potential windows of the solvents limit the applied voltage and frequently induce side reactions, resulting in the deterioration of actuators. Further, ionic EAP actuators with an EDLC structure, which are driven by electric double layer charging and discharging with no redox reactions, appear to possess significant advantages in terms of the simplicity and durability of actuator structures.

There may be two possible ways of creating ionic EAP actuators that can be operated under open atmosphere and even under vacuum. One is through the use of ionic liquids (ILs) because of their nonvolatility and electrochemical stability.[7−11] Actually, polymer electrolytes containing ILs (ion gels)[7,8] are gaining importance as ionic conductors of electrochemical devices,[12] as dielectric layers of organic transistors,[13] and membranes for gas separation[14] as well as for use in catalytic reactions.[15] ILs generally consist of weakly coordinating cations and anions,[16] and thus the interaction between ILs and matrix polymers appears to be weak.[17] Conventional polymer electrolytes,[18] which generally consist of polyethers and lithium salts, are another choice. The polyethers in the polyether electrolytes serve as solvents and aid the dissociation of salts by relatively strong ion-dipole interactions with the cations. As a result, cationic diffusion is coupled with the segmental motion of the polymer, and cationic transference numbers for polyether electrolytes are generally very low.[19] Thus, the ionic transport mechanisms in the ion gels and polyether electrolytes are distinctly different, as was previously proposed.[20]

Polyethers such as poly(ethylene oxide) (PEO) can be host polymers for ILs (the ion gels)[7,21−23] and lithium salts (the conventional polymer electrolytes) because of their high compatibility with these salts.[18] Physically cross-linked polymer

Received: February 14, 2012
Revised: April 6, 2012
Published: April 10, 2012

networks utilizing self-assembled block copolymers are commonly used for polyether membranes with good processability.[24,25] PEUUs are a typical thermoplastic elastomer based on multiblock copolymers consisting of hard polyurethaneurea segments and soft polyether segments. The hard segments and the soft segments of PEUU are microscopically phase-separated and doped salts can be selectively dissolved in the polyether. Thus, if the soft polyether segments form a continuous phase, salt-doped (either an IL or a lithium salt) PEUUs can work as ion-conductive polymer electrolytes with high mechanical strength.[25] To reduce the crystallinity of PEO and enhance chain dynamics, copolymers of ethylene oxide (EO) and 2-(2-methoxyethoxy)ethyl glycidyl ether (MEEGE) were used in this study as the polyether segments of the PEUUs, with the short flexible ether side chains attached to the polyether main chain contributing to fast ionic transport.[26]

The main aim of this study is to propose a model of EDLC polymer actuators for clarifying their driving mechanisms by focusing on the ionic transport phenomena in the polymer electrolytes. In this model, a volume change of the electrode layers gives rise to the deformation of an EDLC polymer actuator, which is caused by the imbalance in the volume and number of ions flowing into and out of the electrode layer. Thus, ionic mobility is a crucial factor in understanding volume change. PGSE-NMR was used to estimate the self-diffusion coefficient of the ions in the electrolytes. The cationic transference numbers of Li[NTf_2] in the polyether were ca. 0.2, whereas the cationic transference numbers of [C_2mim][NTf_2] in the polyether were higher than 0.5. Accordingly, on the basis of our model, actuators using either PEUU/Li[NTf_2] or PEUU/[C_2mim][NTf_2] electrolytes were expected to exhibit opposite deformation behavior. The experimentally obtained actuation behavior could be well-explained on the basis of our proposed model. Our model is supported by a proposal by Asaka and Terasawa et al., who pointed out the importance of the ionic volume of ILs in gel electrolytes in understanding the driving mechanisms of another EDLC actuator, i.e., the bucky gel actuator.[27]

EXPERIMENTAL SECTION

Materials. Potassium naphthalenide solution was prepared using the procedure described in the literature.[28] Sublimed solid naphthalene was charged in a dried round-bottom flask under a N_2 atmosphere, followed by the addition of dry tetrahydrofuran or dry dimethoxyethane. Solid potassium was added to the clear solution portionwise and the solution was stirred at 0 °C overnight. The resultant potassium naphthalenide solution was stored in a refrigerator after the N_2 gas was purged. The concentration of this stock solution was determined by titration using aqueous hydrochloric acid. MEEGE was synthesized using the procedure described in the literature.[26] Poly(ethylene glycol) (PEG, M_n = 298, M_w/M_n = 1.2) was purchased from Aldrich and was dried by azeotropic dehydration with toluene. Methylenediphenyl-4,4′-diisocyanate (MDI) was purchased from TCI and was vacuum distilled at 130 °C/1 mmHg. *trans*-2,5-Dimethylpiperazine (DMP) was purchased from TCI and was purified by recrystallization from acetone. Acetylene black (AB) and activated carbon (AC) were kindly supplied by Denki Kagaku Kogyo and Kuraray Co., Ltd., respectively.

Synthesis. P(EO-*co*-MEEGE) glycol was synthesized by anionic ring-opening polymerization of the epoxide monomers, as shown in Scheme 1. The typical procedure is as follows: 5.9 g

Scheme 1. Synthesis of P(EO-*co*-MEEGE)

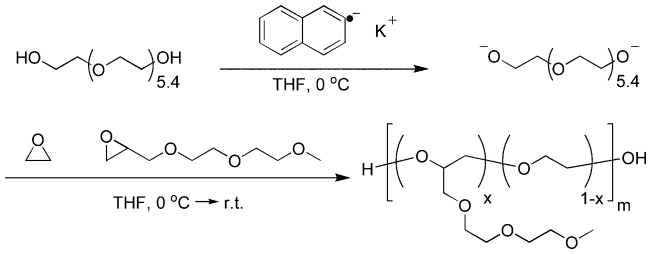

(20 mmol) of PEG and dry tetrahydrofuran (THF, 200 mL) were added to a N_2 purged round-bottom three-necked flask. The flask was cooled in an ice bath and 0.17 L (40 mmol) of 0.24 M potassium naphthalenide solution was added and stirred for 1 h. 60 mL (0.36 mol) of MEEGE and 40 mL (0.81 mol) of EO were added and stirred for about two days, during which the temperature of the reaction mixture gradually increased to room temperature. The conversion of MEEGE was greater than 99.5%, as determined by gas chromatography. The reaction was quenched by the addition of 1 M hydrochloric acid. The THF was evaporated, followed by the addition of dichloromethane and the precipitates were then removed by filtration. The filtrate was washed with saturated sodium chloride solution three times, followed by solvent evaporation. The remaining viscous liquid was washed with hexane four times, and then the liquid was diluted with toluene. The solution was stirred in the presence of an adsorption agent KW-2000 (Kyowa Chemical Industry) for 3 h to remove ionic impurities. The adsorption agent was removed by Celite supported filtration. The filtrate was dried at 80 °C under vacuum for one day (yield 82%). The hydroxyl value of the product was determined by titration and M_n was calculated from the hydroxyl value. The polydispersity index (M_w/M_n) was evaluated by means of gel permeation chromatography (GPC, eluent: *N*,*N*-dimethylformamide with 0.01 M lithium bromide, column: Shodex LF-804) calibrated using PEG standards. The copolymer composition was determined from a ^{1}H NMR spectrum. We prepared two different molecular weight P(EO-*co*-MEEGE) glycols (PE1 and PE2). The molecular weights and monomer compositions are shown in Table 1.

Table 1. Synthetic Results for P(EO-*co*-MEEGE)

	M_n (kg mol^{-1})	M_w (kg mol^{-1})	M_w/M_n	[EO]/[MEEGE]
PE1	5.04	6.00	1.19	74/26
PE2	3.42	4.24	1.24	74/26

PEUUs were synthesized using two-step reactions, as shown in Scheme 2. The typical procedure is as follows: 14.8 g (2.94 mmol) of PE1 was added to a round-bottom four-necked flask and was dried under vacuum at 70 °C for more than 10 h. The flask was filled with N_2 gas and then Et_3N (100 μL) and MDI (4.339 g, 17.36 mmol) were added and stirred by a mechanical stirrer at 30 °C for 3 h. After the addition of 300 mL of *N*, *N*-dimethylacetamide (DMAc), the solution was cooled to −15 °C. DMP (1.644 g, 14.42 mmol) dissolved in 80 mL of DMAc was added dropwise. The chain extension reaction continued for 3 h. The resulting highly viscous solution was added to a large excess amount of diethyl ether. The precipitates were washed by means of Soxhlet extraction using diethyl ether, followed by vacuum drying. An elastic pale-yellow solid was obtained in >95% yield. The polymerization results are shown

dx.doi.org/10.1021/jp301501c | J. Phys. Chem. B 2012, 116, 5080−5089

Scheme 2. Synthesis of PEUU

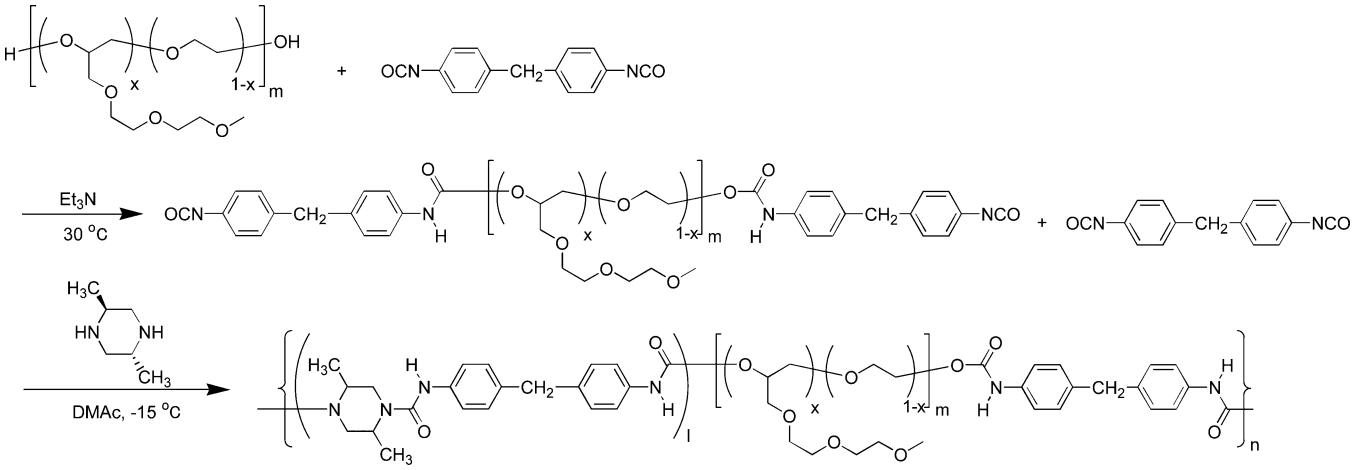

in Table 2. The M_n, M_w, and M_w/M_n values were measured by GPC using polystyrene standards. The weight fraction of the polyurethaneurea segment f_{PUU} (hard segment) was determined from ^{1}H NMR.

Table 2. Synthetic Results for PEUU

	P(EO-*co*-MEEGE)	M_n (kg mol^{-1})	M_w (kg mol^{-1})	M_w/M_n	f_{PUU}
PEUU1	PE1	44.4	114	2.57	0.28
PEUU2	PE2	43.2	78.8	1.82	0.40

Preparation of Polymer Electrolytes. Li[NTf$_2$]-based polymer electrolytes were prepared using PEUU1 (Table 2), which was dissolved in DMAc at a concentration of 5 wt % followed by addition of a given amount of Li[NTf$_2$]. The solution was cast into a flat Petri dish and was dried in air on a hot plate set at 60 °C for two days. The film was dried in a vacuum oven at 80 °C for 2 days to ensure complete solvent removal. Pure PEUU films were prepared using a similar procedure to that described above. [C$_2$mim][NTf$_2$]-based polymer electrolytes were prepared using PEUU2 (Table 2). PEUU2 films were soaked in 5, 10, 20, and 50 vol % [C$_2$mim][NTf$_2$] solutions in acetone for more than 12 h. The film was taken out of the solution and dried in a vacuum oven at 80 °C for two days. PE/salt solutions were prepared by direct dissolution of the salts into the PE and were dried under vacuum at 80 °C for 1 day.

Characterization of Materials. Differential scanning calorimetry (DSC) was performed using a DSC 6220 (SII NanoTechnology Inc.). The sample was put in an aluminum pan under argon atmosphere. The sample pan was cooled from ambient temperature to −150 °C and then the pure PEUU film was heated up to 300 °C, whereas the other samples were heated up to 250 °C, using a scan rate of 10 °C min^{-1} for each process.

Ionic conductivity was measured by means of the complex impedance method using a Hewlett-Packard 4192A impedance analyzer at an oscillation voltage of 10 mV. The measurements were taken every 10 °C and carried out in a temperature range from +100 to −20 °C.

Self-diffusion coefficients for the ions were measured by means of the PGSE-NMR technique using the modified Hahn spin−echo sequence.[29,30] The measurements were performed using a method similar to that described in our previous literature.[31] A sine gradient pulse with a gradient strength of up to 9 T m^{-1} was used throughout the measurement.[31] The samples were inserted into a NMR microtube (BMS-005J, Shigemi, Tokyo) with an outer diameter of 5 mm in the glovebox to a height of 5 mm.

Preparation of Actuators. The actuators have a trilaminar structure that consists of outer electrode layers and an inner electrolyte layer. The outer carbon electrode film was composed of 10 wt % of AB, 20 wt % of AC, and 70 wt % of each polymer electrolyte. The mixed carbon powder was dispersed in DMAc using a planetary centrifugal mixer AR-250 (THINKY). A given amount of a polymer electrolyte solution in DMAc was added to the carbon dispersion. The dispersion was coated onto an aluminum foil and then dried under conditions similar to those used in the preparation of PEUU films. The electrode film was ca. 20 μm thick. Two carbon electrodes were thermally adhered to a ca. 100-μm-thick electrolyte film above 100 °C. The trilaminar films were cut into rectangular shapes having a width of 2 mm and a length of 7 mm to make an actuator element. The final thickness of the electrolyte and electrodes was observed by scanning electron microscopy (SEM) using a HITACHI High-Technologies S-2600N after gentle sputtering of Pt−Pd.

Actuator Performance. An actuator element was clamped by two current collectors made of stainless steel and connected to a potentiostat HA-301 and a function generator HB-104 (HOKUTO DENKO). The displacement was measured by a laser displacement meter LC-2400 (KEYENCE) at 4 mm from the clamped end. In this study, an average of half values of peak-to-peak positions was defined as the displacement value. Displacement measurement was carried out by applying rectangular waveform voltages of ±0.5 to ±4.0 V at a frequency of 0.005 Hz.

RESULTS AND DISCUSSION

Preparation of Polymer Electrolytes. PEUU/Li[NTf$_2$] electrolytes with molar ratios of lithium to ether oxygen ([Li]/[O]) up to 0.10 (Table 3) were prepared as transparent, tough, and elastic films, as shown in Supporting Information, Figure S1. PEUU/[C$_2$mim][NTf$_2$] electrolytes with IL weight fractions up to 0.87 (Table 4), similar in appearance to those of the PEUU/Li[NTf$_2$] electrolytes, were also successfully prepared by changing the [C$_2$mim][NTf$_2$] concentrations of the soaking solutions. All of the PEUU/[C$_2$mim][NTf$_2$]

dx.doi.org/10.1021/jp301501c | J. Phys. Chem. B 2012, 116, 5080−5089

Table 3. Molar Ratio of Lithium to Ether Oxygen ([Li]/[O]), Salt Concentration, T_g of Soft Segments, and T_m of Hard Segments for PEUU/Li[NTf$_2$] Electrolytes

[Li]/[O] molar ratio	C_{salt} (mol kg^{-1})	soft segment T_g (°C)	hard segment T_m (°C)
0	0	−62	254
0.025	0.49	−41	n.d.
0.050	0.86	−24	202
0.075	1.1	−20	203
0.10	1.4	−10	213

Table 4. [C$_2$mim][NTf$_2$] Weight Fraction, Salt Concentration, T_g of Soft Segments, and T_m of Hard Segments for PEUU/[C$_2$mim][NTf$_2$] Electrolytes

[C$_2$mim][NTf$_2$] weight fraction	C_{salt} (mol kg^{-1})	soft segment T_g (°C)	hard segment T_m (°C)
0	0	−59	260
0.13	0.51	−51	199
0.46	1.5	−54	200
0.69	2.0	−61	208
0.87	2.3	−85	181
1.00	2.6	−90	−

electrolyte films were self-standing and no [C$_2$mim][NTf$_2$] leakage was observed, owing to high compatibility between the IL and the polyether segments. It was presumed that the added electrolytes for both PEUU/Li[NTf$_2$] and PEUU/[C$_2$mim][NTf$_2$] electrolytes were selectively dissolved in the polyether segments owing to their preferential affinity. The molar concentration of each salt, C_{salt} (mol kg^{-1}), was calculated by excluding the weight of the polyurethaneurea segment. The salt concentration in the soft polyether domains was calculated by

$$C_{salt} = \frac{w_{salt}/M_{salt}}{w_{salt} + w_{polyether}} = \frac{w_{salt}/M_{salt}}{w_{salt} + w_{PEUU}(1 - f_{PUU})} \quad (1)$$

where w_{salt} is the weight of the salt, M_{salt} is the molar mass of the salt, $w_{polyether}$ is the weight of polyether, and w_{PEUU} is the weight of the PEUU (Tables 2, 3, and 4).

Microstructures of Polymer Electrolytes. The PEUU electrolytes may form microphase-separated structures, caused by incompatibility of the soft polyether segments and the hard polyurethaneurea segments. Furthermore, the microphase-separated structures are affected by the solubility of each salt in the polyether, P(EO-*co*-MEEGE). The thermal properties of the soft segments may greatly depend on the salt compositions because of the selective solubility of Li[NTf$_2$] and [C$_2$mim][NTf$_2$] toward P(EO-*co*-MEEGE), whereas there may be little effect on the hard segments.

The heat capacity change, caused by the glass transition of the soft segments consisting of P(EO-*co*-MEEGE) and either Li[NTf$_2$] or [C$_2$mim][NTf$_2$], of each sample was detected from DSC measurements. No melting transition corresponding to the soft segments was observed for all of the polymer electrolytes, indicating that the P(EO-*co*-MEEGE) soft segment phases are completely amorphous. In this study, we define a glass transition temperature (T_g) as a peak of a differential DSC curve. Moreover, there were endothermic peaks caused by the melting temperature (around 200 °C) of the crystalline polyurethaneurea segments. Tables 3 and 4 summarize salt concentration and thermal properties determined from the DSC measurements of the PEUU/Li[NTf$_2$] and PEUU/[C$_2$mim][NTf$_2$] electrolytes.

Figure 1 shows salt concentration dependencies of T_gs for the PEUU/Li[NTf$_2$] and PEUU/[C$_2$mim][NTf$_2$] electrolytes.

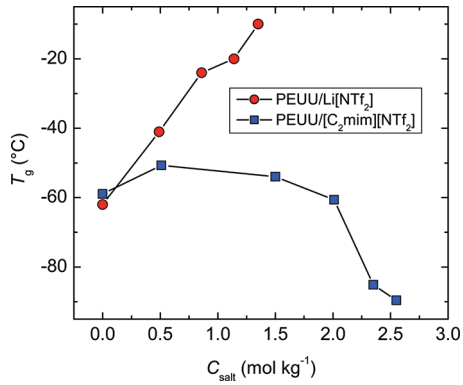

Figure 1. Salt concentration dependence of T_g for PEUU/[C$_2$mim][NTf$_2$] and PEUU/Li[NTf$_2$] determined by DSC.

The T_gs of PEUU/Li[NTf$_2$] electrolytes strongly depend on Li[NTf$_2$] concentrations, compared with those of the PEUU/[C$_2$mim][NTf$_2$] electrolytes, and monotonically increase with increasing Li[NTf$_2$] concentrations. The T_g of pure PEUU is −62 °C and T_g is enhanced up to −10 °C at C_{salt} = 1.4 mol kg^{-1} ([Li]/[O] = 0.1).

Such an increase in T_g is commonly observed for lithium salt/polyether systems[1] and is caused by strong ion-dipole interactions between the ether oxygen atoms and the cations, which work as transient cross-linking points. On the other hand, because of weak Lewis acidity of the [C$_2$mim] cation and weak Lewis basicity of the [NTf$_2$] anion, T_gs of PEUU/[C$_2$mim][NTf$_2$] electrolytes are relatively low. However, the salt concentration dependency of T_g for the PEUU/[C$_2$mim][NTf$_2$] electrolytes changes in a rather complicated manner, compared to that of the PEUU/Li[NTf$_2$] electrolytes. At low salt concentrations, T_gs of the PEUU/[C$_2$mim][NTf$_2$] electrolytes increase slightly with ionic liquid concentration. They decrease to −90 °C of the pure IL after reaching a maximum value, with further increases in [C$_2$mim][NTf$_2$] concentrations. A similar phenomenon was also confirmed for the P(EO-*co*-MEEGE) (PE2)/[C$_2$mim][NTf$_2$] mixture (see Figure S2, Supporting Information). Angell et al.[32] suggested that such a T_g maximum in polyether and glass forming lithium salt systems indicates the transition from salt-in-polymer electrolytes to polymer-in-salt electrolytes. The composition dependency of T_gs in the present system appears to be caused by two opposite effects. One is the plasticization effect of the ionic liquid toward the P(EO-*co*-MEEGE) segment. Generally, T_gs of compatible binary systems monotonically change in accordance with their compositions, and the T_gs of the composites are located between T_gs of the pure components. T_gs of the P(EO-*co*-MEEGE) segment and [C$_2$mim][NTf$_2$] are −59 and −90 °C, respectively (Table 4). Another effect is pseudo cross-linking caused by the interaction between the polyether and the imidazolium cation, leading to T_g elevation. The [C$_2$mim] cations have acidic protons on their imidazolium rings that interact with Lewis basic ether oxygen atoms through hydrogen bonds.[28,33] The importance of hydrogen bonding interaction to the compatibility of polyethers and imidazolium-based ionic liquids was reported in detail.[28,33] The cross-linking effect by

dx.doi.org/10.1021/jp301501c | J. Phys. Chem. B 2012, 116, 5080−5089

hydrogen bonds appears to be predominant at low [C_2mim][NTf_2] concentrations and is accompanied by a slight increase in T_g, whereas at high concentrations, the plasticizing effect overwhelms the hydrogen bonding and causes a decrease in T_g.

It is interesting to note that the T_ms of the polyurethaneurea segments (hard segments) tend to decrease with increasing salt concentrations for both electrolytes (Tables 3 and 4). Although completely preferential dissolution of Li[NTf_2] and [C_2mim][NTf_2] in the polyether soft segments is assumed, these salts may also interact with the polyurethaneurea segments and may reduce crystallinity. Such an interaction also causes a partial mixing of the microphase separation between the soft polyether and the hard polyurethaneurea segments at the interfaces. These effects both lower the T_ms.

Ionic Conductivity. Figures 2 and 3 show Arrhenius plots of ionic conductivity for the PEUU/Li[NTf_2] and PEUU/[C_2mim][NTf_2] electrolytes, respectively. The ionic conductivities at 25 °C reach 1.4×10^{-6} S cm^{-1} for the PEUU/Li[NTf_2] electrolytes and 3.4×10^{-3} S cm^{-1} for the PEUU/[C_2mim][NTf_2] electrolytes. The ionic conductivities of both electrolytes fit the following VTF equation ($R^2 > 0.999$). The VTF fitting parameters are shown in the Supporting Information, Tables S1 and S2.

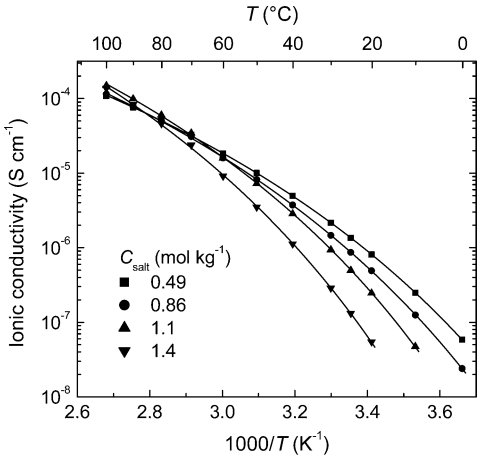

Figure 2. Arrhenius plots of ionic conductivities for PEUU/Li[NTf_2] electrolytes with different Li[NTf_2] concentrations.

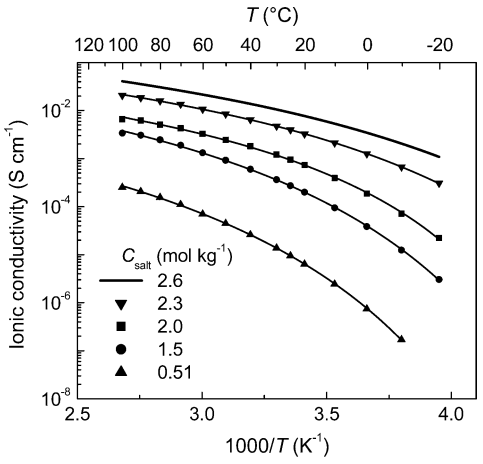

Figure 3. Arrhenius plots of ionic conductivities for PEUU/[C_2mim][NTf_2] electrolytes with different [C_2mim][NTf_2] concentrations.

$$\sigma = \sigma_0 \exp\left(\frac{-B}{T - T_0}\right) \quad (2)$$

The magnitude and the temperature dependence of the ionic conductivities are clearly different in these polymer electrolytes. The difference reflects the differences in ionic transport mechanisms and in the ion transporting role of polyether.[20] The lithium ions in PEUU need strong solvation for the dissociation of Li[NTf_2], and therefore, lithium ion transport is synchronized with polyether segmental motion.[20] This synchronized motion of lithium ions with segmental motion causes lower ionic conductivities and larger temperature dependences. In contrast, the interaction between the ether oxygen and the soft imidazolium cation is much weaker than that of PEUU/Li[NTf_2] electrolytes. As a result, ion transport in PEUU/[C_2mim][NTf_2] electrolytes is decoupled from the segmental motion of the polyether segments.[20] Strong interactions between the polyether solvents and the ions are not necessary for ion dissociation because ionic liquids are self-dissociative.

Such differences in ionic conduction mechanisms affect the salt concentration dependencies of ionic conductivity. As shown in Figure 4, the ionic conductivities of the PEUU/Li[NTf_2] electrolytes gradually decrease with salt concentration or remain at a similar level. On the other hand, the ionic conductivities of the PEUU/[C_2mim][NTf_2] electrolytes greatly increase with salt concentration. These results indicate that both ionic concentration and mobility in PEUU/[C_2mim][NTf_2] electrolytes increase with addition of ionic liquid; however, ionic mobility in PEUU/Li[NTf_2] electrolytes is depressed by lithium salt doping.

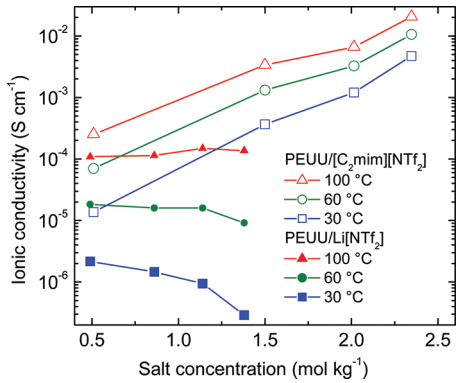

Figure 4. Salt concentration dependencies of ionic conductivities of PEUU-based electrolytes.

Ionic Diffusivity and Transport Mechanism in Polymer Electrolytes. The self-diffusion coefficients of the ions in the polymer electrolytes should provide indispensable information about their ion transport mechanisms. They were therefore measured by means of PGSE-NMR. ^{1}H, ^{7}Li, and ^{19}F NMR were used to determine the diffusion coefficients of [C_2mim]$^+$, Li^+, and [NTf_2]$^-$, respectively. To facilitate the discussion of the ionic transport mechanism, these diffusivities of the PE-based electrolytes, which do not contain polyurethaneurea (hard) segments serving as cross-linking points, were measured (Table 1) because the diffusion coefficients of the ions in the PEUU-based electrolytes were too low to be measured by our PGSE-NMR system. The mechanical strength of the PEUU electrolytes also caused difficulty in preparing NMR samples. It

dx.doi.org/10.1021/jp301501c | J. Phys. Chem. B 2012, 116, 5080−5089

is assumed that the ionic transport mechanisms in the PEUU-based electrolytes are essentially the same as in the PE electrolytes.

The self-diffusion coefficients (D) and cationic transference numbers (t_+) of the PE/Li[NTf_2] and PE/[C_2mim][NTf_2] electrolytes are listed in Table 5 and Table 6, respectively. We

Table 5. Self-Diffusion Coefficients and Cationic Transference Numbers for PE1/Li[NTf_2] Electrolytes Determined by PGSE-NMR Measurements

[Li]/[O] molar ratio	C_{salt} (mol kg^{-1})	T (°C)	D (10^{-11} m^2 s^{-1}) D_+ (^{7}Li)	D (10^{-11} m^2 s^{-1}) D_- (^{19}F)	t_+
0.025	0.49	60	0.43	1.6	0.21
0.025	0.49	80	0.95	3.3	0.22
0.050	0.86	60	0.23	0.98	0.19
0.050	0.86	80	0.54	2.2	0.20

Table 6. Self diffusion coefficients and cationic transference numbers for PE2/[C_2mim][NTf_2] electrolytes determined by PGSE-NMR measurements at 30°C

[C_2mim][NTf_2] weight fraction	C_{salt} (mol kg^{-1})	D (10^{-11} m^2 s^{-1}) D_+ (^{1}H)	D (10^{-11} m^2 s^{-1}) D_- (^{19}F)	t_+
0.20	0.51	1.1	0.90	0.55
0.40	1.0	1.3	0.92	0.58
0.60	1.5	1.8	1.2	0.60
0.80	2.0	3.3	2.0	0.62
1.0	2.6	6.2	3.7	0.63

assume that the diffusivities (D) can be correlated with the ionic mobilities (u) by Nernst−Einstein relation:

$$u = \frac{|z|qD}{k_B T} \tag{3}$$

where z is valence of ion, q is elementary charge, k_B is the Boltzmann constant, and T is the absolute temperature. For completely dissociated electrolytes consisting of monovalent cation and anion, the cationic transference numbers are defined from the self-diffusion coefficients for the cation (D_+) and anion (D_-) as follows:

$$t_+ = \frac{D_+}{D_+ + D_-} = 1 - t_- \tag{4}$$

From the cationic and anionic diffusion coefficients, the densities and the ionic conductivities, dissociativity ($\Lambda_{imp}/\Lambda_{NMR}$) of Li[$NTf_2$] and [$C_2$min][$NTf_2$] in the PE based electrolytes were estimated,[31] where Λ_{imp} is the molar conductivity evaluated from impedance measurement and Λ_{NMR} is from the diffusivities by the PGSE-NMR measurements. The $\Lambda_{imp}/\Lambda_{NMR}$ of PE/Li[NTf_2] is as high as 0.9, and that of PE/[C_2min][NTf_2] (= 0.74) is similar to that of pure [C_2min][NTf_2] (= 0.77), as shown in Supporting Information (Table S3). These results suggest that the ions in the PE-based electrolytes are highly dissociated and that the application of eqs 3 and 4 to the present system is appropriate.

The temperatures had to be elevated when measuring the ionic diffusivities of the PE/Li[NTf_2] electrolytes because of low ionic diffusivity. As shown in Table 5, the t_+ values are found to be ca. 0.2 and are barely affected by the temperatures of the PE/Li[NTf_2] electrolytes, which is approximately consistent with the t_+ value in high molecular weight P(EO-*co*-MEEGE).[19] In contrast, the t_+ values of the PE/[C_2mim][NTf_2] electrolytes (Table 6) depend on [C_2mim][NTf_2] concentrations; the t_+ values of pure [C_2mim][NTf_2] (t_+ is 0.63) decrease with decreasing [C_2mim][NTf_2] concentrations. The difference in the t_+ values of PE/Li[NTf_2] and PE/[C_2mim][NTf_2] reflects the strength of the interaction between the cations and the ether oxygen (*vide supra*). Highly Lewis acidic Li^+ interacts with oxygen atoms on the polyether chains and the interaction aids the dissociation of Li[NTf_2] and simultaneously confines the free motion of the Li^+ ions, in contrast to relatively free $[NTf_2]^-$. $[C_2mim]^+$ also interacts with the polyether, which induces lower t_+ values compared with pure [C_2mim][NTf_2]; however, the interaction is much weaker than the Li^+−O interactions.

Deformation Model for Actuators Having EDLC Structures. A deformation model based on the ion transport mechanism of the polymer electrolytes was formulated for the actuators in this study; the actuators have a trilaminar structure consisting of outer electrode layers and an inner polymer electrolyte layer and are a type of solid EDLC. A voltage application induces ionic currents, where cations and anions flow into and out of a cathodic and an anodic electrolyte layer, respectively. The major electrode materials used in this study are high-surface-area AC powders. The polarized ions cannot discharge at the electrode | electrolyte interfaces under our experimental conditions and form electric double layers at the interfaces. The electrolyte layer is composed of a physically cross-linked polyether phase with a dissolved salt and contains no low molecular solvents. Therefore, only mass transport of ions is considered. It is assumed that volume changes of electrodes induce deformation and occur only by ionic transport phenomena. Volume change caused by redox reactions, as seen in conducting-polymer-based actuators,[4] and the quantum chemical effect, as proposed in carbon nanotube-based actuators, are ignored.[6]

The contribution of the ionic species, J, to the cathodic volume change, ΔV_J, is the product of the volume of J and its number change in the cathodic layer and is given by

$$\Delta V_J = \frac{Qt_J}{qz_J}v_J \tag{5}$$

where Q is the charge stored at the double layer (the integration of ionic current), t_J is the transference number of J, z_J is the valence of J, and v_J is the volume of J. The total volume change of cathode, ΔV, is derived from the sum of ΔV_J, written as

$$\Delta V = \frac{Q}{q}\sum_J \frac{t_J v_J}{z_J} \tag{6}$$

Electrolyte salts used in this study consist of a monovalent cation and a monovalent anion. Hence, eq 6 can be simplified to

$$\Delta V = \frac{Q}{q}(t_+ v_+ - t_- v_-) \tag{7}$$

where t_+ is the cationic transference number, v_+ is the cationic volume, t_- is the anionic transference number, and v_- is the anionic volume. An anodic volume change also occurs and equals $-\Delta V$. The sign of ΔV depends on the magnitude of the products of the transference number and ionic volume.

dx.doi.org/10.1021/jp301501c | J. Phys. Chem. B 2012, 116, 5080−5089

The relationship between the strain of the electrode, ε, and ΔV is given by

$$\varepsilon = \left(1 + \frac{\Delta V}{V_0}\right)^{1/3} - 1 \tag{8}$$

where V_0 is the initial volume of the electrode. If $\Delta V/V_0$ is sufficiently small, eq 8 can be approximated using a linear approximate relationship around the origin, $f(\Delta V/V_0) \approx f(0) + f'(0) \times \Delta V/V_0$:

$$\varepsilon = \frac{\Delta V}{3V_0} \tag{9}$$

By substituting eq 9 into eq 7, the relationship between ε and Q can be obtained:

$$\varepsilon = \frac{Q}{3qV_0}(t_+\nu_+ - t_-\nu_-) \tag{10}$$

To obtain the relationship between the displacement of the actuator, d, and ΔV, it is assumed that the deformation curvature of the actuator is constant (Figure 5). This

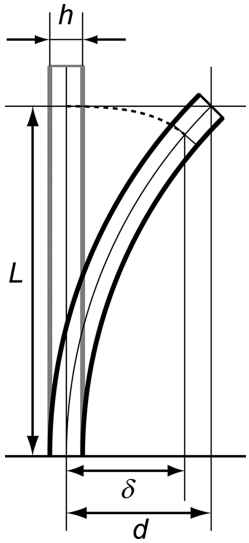

Figure 5. Illustration representing the shape and deformation of an actuator with a trilaminar structure consisting of outer electrode layers and an inner polymer electrolyte layer.

assumption needs the conditions that the ionic charge passing through the electrolyte layer is homogeneous from the root to the tip of the actuator. ε is calculated from eq 11:

$$\varepsilon = \frac{hd}{L^2 + d^2} \tag{11}$$

where h and L are the thickness and length of the actuator, respectively. In a precise sense, the measured displacement, δ, is not equal to the tip displacement, d (Figure 5). However, if d is small enough relative to L, d is approximately equal to δ, and the error is almost negligible. The relationship between ε and δ can be described as

$$\varepsilon = \frac{h\delta}{L^2} \tag{12}$$

From eqs 10 and 12, we obtain a simple relationship

$$\delta = \frac{L^2 Q}{3hqV_0}(t_+\nu_+ - t_-\nu_-) \tag{13}$$

The important point is that the direction of the deformation depends on the sign of $t_+\nu_+ - t_-\nu_-$. In other words, the actuators bend to the anodic side when $t_+\nu_+ - t_-\nu_- > 0$, and bend to the cathodic side when $t_+\nu_+ - t_-\nu_- < 0$. The absolute value of $(t_+\nu_+ - t_-\nu_-)/q$ indicates the volume change of the electrode per unit charge. Actuators with electrolytes with large $|t_+\nu_+ - t_-\nu_-|$ may perform the same displacement with a smaller Q. This property is effective for fast motion or low power consumption. Hence, $t_+\nu_+ - t_-\nu_-$ affects both the deformation behavior and performance of the actuator.

Assuming that the ionic transference number of the PEUU-based electrolytes and the PE-based electrolytes is the same, the $t_+\nu_+ - t_-\nu_-$ values for the PEUU electrolytes were estimated from the ionic transference numbers and the ionic volumes. The ionic volumes for Li^+, $[C_2mim]^+$, and $[NTf_2]^-$ have been calculated as 1.8, 116, and 147 Å^3, respectively.[34] The salt concentration, the ionic transference numbers, the ionic volumes, and the $t_+\nu_+ - t_-\nu_-$ values for the PEUU/$[C_2mim][NTf_2]$ and PEUU/$Li[NTf_2]$ electrolytes used in the actuators are summarized in Table 7. From the values in Table

Table 7. Salt Concentration, Ionic Transference Number, Ionic Volume, and $t_+\nu_+ - t_-\nu_-$ for PEUU/$[C_2mim][NTf_2]$ and PEUU/$Li[NTf_2]$ Electrolytes

electrolyte	C_{salt} (mol kg^{-1})	t_+	ν_+ (Å^3)	ν_- (Å^3)	$t_+\nu_+ - t_-\nu_-$ (Å^3)
PEUU/$Li[NTf_2]$	0.86	0.20	1.8	147	−117
PEUU/$[C_2mim][NTf_2]$	2.0	0.62	116	147	16

7, the PEUU/$[C_2mim][NTf_2]$-based actuators are expected to bend to the anodic side, whereas the PEUU/$Li[NTf_2]$-based actuators are expected to bend to the cathodic side. Furthermore, the PEUU/$Li[NTf_2]$-based actuators need only 14% of the ionic charge to perform an equal displacement, in comparison with the PEUU/$[C_2mim][NTf_2]$-based actuators of the same size.

Validity of the Model for Explaining Actuator Deformations. The actuators have a trilaminar structure, but their monolithic structures are very important for stable and durable deformation. A PEUU/$Li[NTf_2]$ actuator was prepared using an electrolyte film with a salt concentration of 0.86 mol kg^{-1} ([Li]/[O] = 0.050). The total thickness of the actuator was 110 μm and the thickness of each electrode was 20 μm. A PEUU/$[C_2mim][NTf_2]$ actuator was prepared using the electrolyte film with a salt concentration of 2.0 mol kg^{-1}. The total thickness of the actuator was 160 μm and the thickness of each electrode was 20 μm. SEM images of these actuator elements, as shown in Figure 6, confirm their monolithic structures as well as the thickness of each layer.

Figure 7 shows current and displacement responses of these actuators against a rectangular waveform voltage (±1.5 V) applied at a frequency of 0.01 Hz. In Figure 7, the positive displacement indicates deformation to the anodic side. A comparison between Figure 7a (PEUU/$Li[NTf_2]$) and Figure 7b (PEUU/$[C_2mim][NTf_2]$) reveals two important features in which the two actuators respond differently to the applied voltage in terms of the current magnitude and the direction of deformation. A charging current is observed at the moment of voltage reversal and then the current exponentially decreases

dx.doi.org/10.1021/jp301501c | J. Phys. Chem. B 2012, 116, 5080−5089

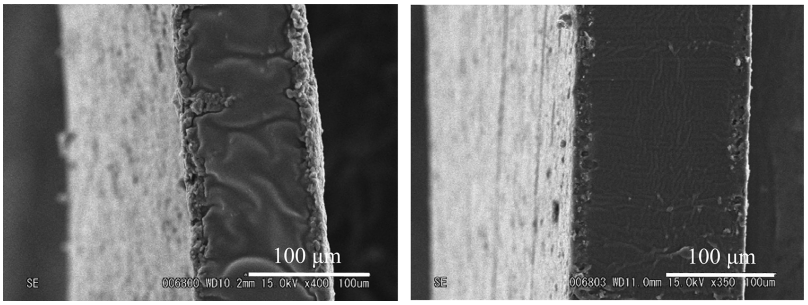

Figure 6. SEM images of the cross-section of the actuators using PEUU/Li[NTf_2] (left) and PEUU/[C_2mim][NTf_2] (right).

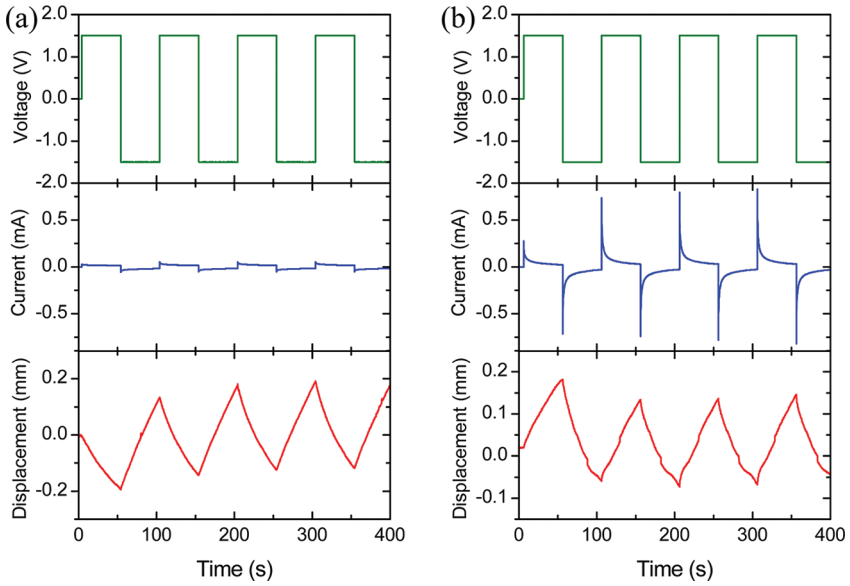

Figure 7. Current and displacement responses of actuators using PEUU/Li[NTf_2] (a) and PEUU/[C_2mim][NTf_2] (b) electrolytes driven by a square waveform voltage of ±1.5 V at a frequency of 0.01 Hz.

with time. A relatively large current is observed for the PEUU/[C_2mim][NTf_2]-based actuator because it has higher ionic conductivity than the PEUU/Li[NTf_2]-based actuator. It takes more than 50 s for the current to completely decay, and consequently, the deformation continues throughout this period. This result suggests that the actuators have long and widely distributed time constants. For common EDLCs, an electrolyte solution is a major component of the resistance because the electrode resistance is much smaller. However, as discussed in our previous paper,[35] the longitudinal resistance of the electrode film is not negligible owing to the low electronic conductivity of the carbon electrode film (ca. 10^{-2} S cm^{-1}). One end of a rectangular trilaminar specimen was clipped between stainless steel current-collectors in the actuation experiments. The carbon electrode layer is much more resistive compared with the metal. Consequently, the potential drop along the longitudinal direction of the actuator specimen cannot be neglected. It takes much longer to complete electric double layer charging at the tip of the actuator element than at its root. This is the main reason for the actuators taking a long time to deform.

It is quite interesting to note that deformation directions of the PEUU/Li[NTf_2] actuator and PEUU/[C_2mim][NTf_2] actuator are different: the cathodic side for the PEUU/Li[NTf_2] actuator and the anodic side for the PEUU/[C_2mim][NTf_2] actuator (Figure 8). These experimental results agree with the prediction based our proposed model.

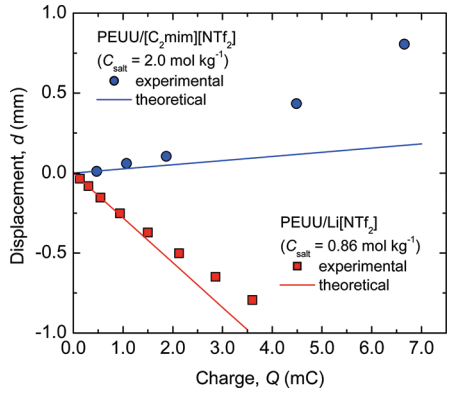

Figure 8. Displacement of actuators with different polymer electrolytes as a function of the ionic charge stored in the actuators. A positive displacement indicates that the tip of the actuator moves to the anodic side. The theoretical lines are calculated from eq 13 and the data in Table 7.

By changing the magnitude of rectangular wave voltages, the relationship between the magnitude of displacement and the double layer charge stored at the electrode | electrolyte interface was estimated. Figure 8 shows the magnitude of displacement as a function of the stored charge calculated by integration of the current, where the plots indicate the experimental results and the theoretical lines are calculated from eq 13 using

dx.doi.org/10.1021/jp301501c | J. Phys. Chem. B 2012, 116, 5080−5089

experimental values for L, Q, h, V_0, t_+, and t_- and reported values of v_+ and v_-.[34] The displacement results based on eqs 10 and 11 give the same result as those based on eq 13, indicating that the assumption of eq 12 in our systems is valid. Figure 8 also clearly shows that the PEUU/Li[NTf_2] actuator gives a larger displacement compared with the PEUU/[C_2mim][NTf_2], as expected from the results in Table 7 and the proposed model (*vide supra*).

The theoretical lines are consistent with the experimental plots within the stored charge range of <2 mC. However, inconsistencies between the experimental data and the calculated data based on our model become apparent at >2 mC. An increase in the stored charge corresponds to an increase in the applied voltage, since it is controlled by the magnitude of applied rectangular wave voltages. Although the details are still not clear, these discrepancies appear to be caused by the effects of the leakage current and nonuniform deformation. These effects may become more noticeable when a larger voltage is applied. The displacement of the PEUU/Li[NTf_2] actuator tends to level off with increasing stored charge, which may be caused by an increase in the leakage current, possibly owing to certain Faradaic reactions. The ionic conductivity of the PEUU/Li[NTf_2] electrolyte is very low (10^{-6} S cm^{-1}), which is reflected in the much smaller charging current compared with that of the PEUU/[C_2mim][NTf_2] electrolyte (Figure 7). This low charging current enlarges the influence of the leakage current. Furthermore, bending displacement induces an elastic force to recover the shape of an actuator to the original (nonbending) shape, which is not taken into consideration during model formulation. The ionic conductivity of the PEUU/[C_2mim][NTf_2] actuators is much higher (10^{-3} S cm^{-1}) and the charging current becomes much larger at the same voltage magnitude, in which case the *iR* drop along the longitudinal electrode direction becomes serious, inducing nonuniform deformation. Specifically, a large volume change at the root of the actuator element owing to the concentration of current at the root may cause a larger displacement at high application voltages than that calculated using the model.

CONCLUSIONS

PEUUs with aromatic polyurethaneurea segments and branched polyether segments were synthesized, forming phase-separated structures between these two segments. Two different polymer electrolytes were prepared by selective incorporation of either Li[NTf_2] or [C_2mim][NTf_2] into the polyether segments. Ionic conductivities reached 1.4×10^{-6} S cm^{-1} for the PEUU/Li[NTf_2] electrolyte and 3.4×10^{-3} S cm^{-1} for the PEUU/[C_2mim][NTf_2] electrolyte. The differences in ionic transport mechanisms between the PEUU/[C_2mim][NTf_2] and PEUU/Li[NTf_2] electrolytes were discussed in terms of ionic conductivities and self-diffusion coefficients. The most striking difference between these two electrolytes is that $t_+ < 0.5$ for the PEUU/Li[NTf_2] electrolyte, whereas $t_+ > 0.5$ for the PEUU/[C_2mim][NTf_2] electrolyte. Taking the difference in the ionic transport mechanisms into consideration, a deformation model for actuators having solid EDLC structures was proposed. The model pointed out the important factor, $t_+v_+ - t_-v_-$, which determines the direction of deformation against applied voltage. The deformation behavior of actuators with either PEUU/Li[NTf_2] or PEUU/[C_2mim][NTf_2] electrolyte were compared using the model. The displacement direction of the actuator agreed with the model: the cathodic side for the PEUU/Li[NTf_2] actuator and the anodic side for the PEUU/[C_2mim][NTf_2] actuator. The magnitude of displacement was in good agreement with the predicted magnitude calculated from the model when the stored charge was small.

ASSOCIATED CONTENT

Supporting Information

Photograph of the PEUU/Li[NTf_2] electrolyte film (Figure S1), glass transition temperatures for PE2/[C_2mim][NTf_2] electrolytes (Figure S2), VTF equation fitting parameters of ionic conductivities for PEUU/Li[NTf_2] and PEUU/[C_2mim][NTf_2] electrolytes (Table S1 and S2), and density and $\Lambda_{imp}/\Lambda_{NMR}$ for PE-based electrolytes (Table S3). This material is available free of charge via the Internet at http://pubs.acs.org.

AUTHOR INFORMATION

Corresponding Author

*Telephone and fax: +81-45-339-3955. E-mail address: mwatanab@ynu.ac.jp.

Notes

The authors declare no competing financial interest.

ACKNOWLEDGMENTS

This work was supported in part by Grants-in-aid for Scientific Research on Priority Areas (No. 438-19016014 and No. 452-17073009) from the MEXT of Japan.

REFERENCES

(1) (a) *Application of Electroactive Polymers*; Scrosati, B., Ed.; Chapman & Hall: London, 1993. (b) *Electroactive Polymer (EAP) Actuators as Artificial Muscles*; Bar-Cohen, Y., Ed.; SPIE Press: Bellingham, WA, 2001.

(2) Pelrine, R.; Kombluh, R.; Pei, Q.; Joseph, J. *Science* **2000**, *287*, 836.

(3) Osada, Y.; Okuzaki, H.; Hori, H. *Nature* **1992**, *355*, 242.

(4) (a) Kaneto, K.; Kaneko, M.; Min, Y.; MacDiarmid, A. G. *Synth. Met.* **1995**, *71*, 2211. (b) Baughman, R. H. *Synth. Met.* **1996**, *78*, 339. (c) Smela, E. *Adv. Mater.* **2003**, *15*, 48.

(5) (a) Asaka, K.; Oguro, K.; Nishimura, Y.; Mizuhata, M.; Takenaka, H. *Polym. J.* **1995**, *27*, 436. (b) Shahinpoor, M. *Electrochim. Acta* **2003**, *48*, 2343.

(6) Baughman, R. H.; Cui, C.; Zakhidov, A. A.; Iqbal, Z.; Barisci, J. N.; Spinks, G. M.; Wallace, G. G.; Mazzoldi, A.; Rossi, D. D.; Rinzler, A. G.; Jaschinski, O.; Roth, S.; Kertesz, M. *Science* **1999**, *284*, 1340.

(7) *Ionic liquids in Polymer Systems: Solvents, Additives, and Novel Applications*; ACS Symposium Series 913; Brazel, C. S., Rogers, R. D., Eds.; American Chemical Society: Washington DC, 2005.

(8) Susan, M. A. B. H.; Kaneko, T.; Noda, A.; Watanabe, M. *J. Am. Chem. Soc.* **2005**, *127*, 4976.

(9) Lu, W.; Fadeev, A. G.; Qi, E.; Smela, B. H.; Mattes, B. R.; Ding, J.; Spinks, G. M.; Mazurkiewicz, J.; Zhou, D. Z.; Wallace, G. G.; MacFarlane, D. R.; Forsyth, S. A.; Forsyth, M. *Science* **2002**, *297*, 983.

(10) (a) Bennett, M. D.; Leo, D. J. *Sens. Actuators A* **2004**, *115*, 79. (b) Akle, B. J.; Bennett, M. D.; Leo, D. J. *Sens. Actuators A* **2006**, *126*, 173.

(11) (a) Fukushima, T.; Asaka, K.; Kosaka, A.; Aida, T. *Angew. Chem., Int. Ed.* **2005**, *44*, 2410. (b) Mukai, K.; Asaka, K.; Kiyohara, K.; Sugino, T.; Takeuchi, I.; Fukushima, T.; Aida, T. *Electrochim. Acta* **2008**, *53*, 5555.

(12) (a) Lewandowski, A.; Świderska, A. *Solid State Ionics* **2003**, *161*, 243. (b) Isshiki, Y.; Nakamura, M.; Tabata, S.; Dokko, K.; Watanabe, M. *Polym. Adv. Tech.* **2011**, *22*, 1254. (c) Shobukawa, H.; Tokuda, H.; Susan, M.; Watanabe, M. *Electrochim. Acta* **2005**, *50*, 3872. (d) Shin, J.-H.; Henderson, W. A.; Passerini, S. *J. Electrochem. Soc.* **2005**, *152*,

A978. (e) Lee, S.-Y.; Ogawa, A.; Kanno, M.; Nakamoto, H.; Yasuda, T.; Watanabe, M. *J. Am. Chem. Soc.* **2010**, *132*, 9764. (f) Wang, P.; Zakeeruddin, S. M.; Exnar, I.; Grätzel, M. *Chem. Commun.* **2002**, 2972.
(13) (a) Lee, J.; Panzer, M. J.; He, Y.; Lodge, T. P.; Frisbie, C. D. *J. Am. Chem. Soc.* **2007**, *129*, 4532. (b) Cho, J. H.; Lee, J.; Xia, Y.; Kim, B.; He, Y.; Renn, M. J.; Lodge, T. P.; Frisbie, C. D. *Nat. Mater.* **2008**, *7*, 900.
(14) (a) Bara, J. E.; Camper, D. E.; Gin, D. L.; Noble, R. D. *Acc. Chem. Res.* **2010**, *43*, 152. (b) Bara, J. E.; Hatakeyama, E. S.; Gabriel, C. J.; Zeng, X.; Lessmann, S.; Noble, R. D. *J. Membr. Sci.* **2008**, *316*, 186.
(15) Scott, K.; Basov, N.; Jachuck, R.; Winterton, N.; Cooper, A.; Davies, C. *Chem. Eng. Res. Des.* **2005**, *83*, 1179.
(16) Ueno, K.; Tokuda, H.; Watanabe, M. *Phys. Chem. Chem. Phys.* **2010**, *12*, 1649.
(17) Bhattacharya, B.; Lee, J. Y.; Geng, J.; Jung, H.-T.; Park, J.-K. *Langmuir* **2009**, *25*, 3276.
(18) (a) *Polymer Electrolyte Reviews 1 and 2*; MacCallum, J. R., Vincent, C. A., Eds.; Elsevier: London, 1987 and 1989. (b) Gray, F. M. *Solid Polymer Electrolytes*; VCH Publishers: New York, 1991.
(19) Tokuda, H.; Tabata, S.; Susan, M. A. B. H.; Hayamizu, K.; Watanabe, M. *J. Phys. Chem. B* **2004**, *108*, 11995.
(20) Seki, S.; Susan, M. A. B. H.; Kaneko, T.; Tokuda, H.; Noda, A.; Watanabe, M. *J. Phys. Chem B* **2005**, *109*, 3886.
(21) Klingshirn, M. A.; Spear, S. K.; Subramanian, R.; Holbrey, J. D.; Huddleston, J. G.; Rogers, R. D. *Chem. Mater.* **2004**, *16*, 3091.
(22) He, Y.; Boswell, P. G.; Bühlmann, P.; Lodge, T. P. *J. Phys. Chem. B* **2007**, *111*, 4645.
(23) Harner, J. M.; Hoagland, D. A. *J. Phys. Chem. B* **2010**, *114*, 3411.
(24) (a) Epps, T. H.; Bailey, T. S.; Waletzko, R.; Bates, F. S. *Macromolecules* **2003**, *36*, 2873. (b) Soo, P. P.; Huang, B.; Jang, Y.-I.; Chiang, Y.-M.; Sadoway, D. R.; Mayes, A. M. *J. Electrochem. Soc.* **1999**, *146*, 32. (c) Jannasch, P. *Chem. Mater.* **2002**, *14*, 2718.
(25) Watanabe, M.; Oohashi, S.; Sanui, K.; Ogata, N.; Kobayashi, T.; Ohtaki, Z. *Macromolecules* **1985**, *18*, 1945.
(26) (a) Nishimoto, A.; Agehara, K.; Furuya, N.; Watanabe, T.; Watanabe, M. *Macromolecules* **1999**, *32*, 1541. (b) Nishimoto, A.; Watanabe, M.; Ikeda, Y.; Kohjiya, S. *Electrochim. Acta* **1998**, *43*, 1177.
(27) (a) Takeuchi, I.; Asaka, K.; Kiyohara, K.; Sugino, T.; Terasawa, N.; Mukai, K.; Fukushima, T.; Aida, T. *Electrochim. Acta* **2009**, *54*, 1762. (b) Terasawa, N.; Takeuchi, I.; Matsumoto, H. *Sens. Actuators B* **2009**, *139*, 624. (c) Terasawa, N.; Takeuchi, I. *Sens. Actuators B* **2010**, *145*, 775.
(28) (a) Tsuda, R.; Kodama, K.; Ueki, T.; Kokubo, H.; Imabayashi, S.; Watanabe, M. *Chem. Commun.* **2008**, 4939. (b) Kodama, K.; Tsuda, R.; Niitsuma, K.; Tamura, T.; Ueki, T.; Kokubo, H.; Watanabe, M. *Polym. J.* **2011**, *43*, 242.
(29) (a) Hayamizu, K.; Aihara, Y.; Arai, S. *J. Phys. Chem. B* **1999**, *103*, 519. (b) Noda, A.; Hayamizu, K.; Watanabe, M. *J. Phys. Chem. B* **2001**, *105*, 4603. (c) Hayamizu, K.; Akiba, E.; Bando, T.; Aihara, Y. *J. Chem. Phys.* **2002**, *117*, 5929.
(30) (a) Hahn, M.; Barbieri, O.; Gallay, R.; Kötz, R. *Carbon* **2006**, *44*, 2523. (b) Hahn, M.; Barbieri, O.; Campana, F. P.; Kötz, R.; Gallay, R. *Appl. Phys. A: Mater. Sci. Process.* **2005**, *82*, 633.
(31) Tokuda, H.; Hayamizu, K.; Ishii, K.; Susan, M. A. B. H.; Watanabe, M. *J. Phys. Chem. B* **2004**, *108*, 16593.
(32) Angell, C. A.; Liu, C.; Sanchez, E. *Nature* **1993**, *362*, 137.
(33) Ueki, T.; Watanabe, M. *Bull. Chem. Soc. Jpn.* **2012**, *85*, 33.
(34) (a) Ue, M. *J. Electrochem. Soc.* **1994**, *141*, 3336. (b) Ue, M.; Murakami, A.; Nakamura, S. *J. Electrochem. Soc.* **2002**, *149*, A1385.
(35) Imaizumi, S.; Kokubo, H.; Watanabe, M. *Macromolecules* **2012**, *45*, 401.